Bioelectrochemistry 140 (2021) 107736

Contents lists available at ScienceDirect

Bioelectrochemistry

journal homepage: www.elsevier.com/locate/bioelechem

Electrochemical studies of the interaction of rifampicin and nanosome/rifampicin with dsDNA

Victoria V. Shumyantseva [a,b,c,*], Tatiana V. Bulko [a,c], Elena G. Tikhonova [a], Maxim A. Sanzhakov [a], Alexey V. Kuzikov [a,b,c], Rami A. Masamrekh [a,b,c], Dmitry V. Pergushov [c], Felix H. Schacher [d,e,f], Larisa V. Sigolaeva [a,c]

[a] Institute of Biomedical Chemistry, Pogodinskaya Street 10, 119121 Moscow, Russia
[b] Pirogov Russian National Research Medical University, Ostrovitianov Street 1, 117997 Moscow, Russia
[c] Department of Chemistry, M.V. Lomonosov Moscow State University, Leninskie Gory 1/3, 119991 Moscow, Russia
[d] Institute of Organic Chemistry and Macromolecular Chemistry (IOMC), Friedrich-Schiller-University Jena, D-07743 Jena, Germany
[e] Jena Center for Soft Matter (JCSM), Friedrich-Schiller-University Jena, D-07743 Jena, Germany
[f] Center for Energy and Environmental Chemistry (CEEC), Friedrich-Schiller-University Jena, D-07743 Jena, Germany

ARTICLE INFO

Article history:
Received 3 August 2020
Received in revised form 21 December 2020
Accepted 23 December 2020
Available online 29 December 2020

Keywords:
Rifampicin
Antibiotic
DNA
Electrochemical biosensor
Amphiphilic diblock copolymer
Phospholipid nanoparticles

ABSTRACT

The interactions of dsDNA with rifampicin (RF) or with rifampicin after encapsulation in phospholipid micelles (nanosome/rifampicin) (NRF) were studied electrochemically. Screen-printed electrodes (SPEs) modified by stable dispersions of multi-walled carbon nanotubes (MWCNTs) in aqueous solution of poly(1,2-butadiene)-*block*-poly(2-(dimethylamino)ethyl methacrylate) (PB_{290}-*b*-$PDMAEMA_{240}$) diblock copolymer were used for quantitative electrochemical investigation of direct electrochemical oxidation of guanine at E = 0.591 V (vs. Ag/AgCl) and adenine at E = 0.874 V (vs. Ag/AgCl) of dsDNA and its change in the presence of RF or NRF. Due to RF or NRF interaction with dsDNA, the differential pulse voltammetry (DPV) peak currents of guanine and adenine decreased and the peak potentials shifted to more positive values with increasing drug concentration (RF or NRF). Binding constants (K_b) of complexes RF-dsDNA and NRF-dsDNA were calculated based on adenine and guanine oxidation signals. The K_b values for RF-dsDNA were 1.48×10^4 M^{-1}/8.56×10^4 M^{-1}, while for NRF-dsDNA were 2.51×10^4 M^{-1}/1.78×10^3 M^{-1} (based on adenine or guanine oxidation signals, respectively). The values of K_b revealed intercalation mode of interaction with dsDNA for RF and mixed type of interaction (intercalation and electrostatic mode) for NRF. The estimated values of ΔG (Gibbs free energy) of the complex formation confirmed that drug-dsDNA interactions are spontaneous and favourable reactions.

1. Introduction

Rifampicin (3-([(4-Methyl–1–piperazinyl) imino] methyl) rifamycin) (RF) exhibits anti-microbial as well as anti-viral activity [1]. RF contains two condensed aromatic moieties, which are connected by a long aliphatic chain in a basket-like manner of molecular architecture (Scheme 1).

RF is an important member of ansamycin family, it is a well-known anti-mycobacterial agent, which is widely used to treat pulmonary diseases and serious infectious such as tuberculosis, leprosy and HIV as part of the combined therapy approach recommended by the World Health Organization. It has been classified as a first line drug characterized as highly effective, orally administered and non-toxic compound [2–5]. Despite the adverse effects such as nausea, hepatotoxicity, and allergic rashes, RF has been widely used for the treatment of various bacterial infections because it is more effective antibiotic than other antibiotics like isoniazid [3]. It was shown recently that RF possesses photonuclease activity towards DNA and supposed to be a potential anticancer agent [5].

However, RF has been reported to cause some severe side effects related to its pharmacokinetics. To overcome such adverse effects, polymeric scaffolds as drug delivery systems for the encapsulation of RF were developed [6,7]. Drug delivery systems based

Abbreviations: RF, rifampicin; NRF, rifampicin/phospholipids drug delivery system (nanosome/rifampicin); SPE, screen-printed electrode; dsDNA, double stranded DNA; A, adenine; GG, guanine.

* Corresponding author at: Institute of Biomedical Chemistry, Pogodinskaya Street, 10, Moscow 119121, Russia.
E-mail address: viktoria.shumyantseva@ibmc.msk.ru (V.V. Shumyantseva).

https://doi.org/10.1016/j.bioelechem.2020.107736
1567-5394/

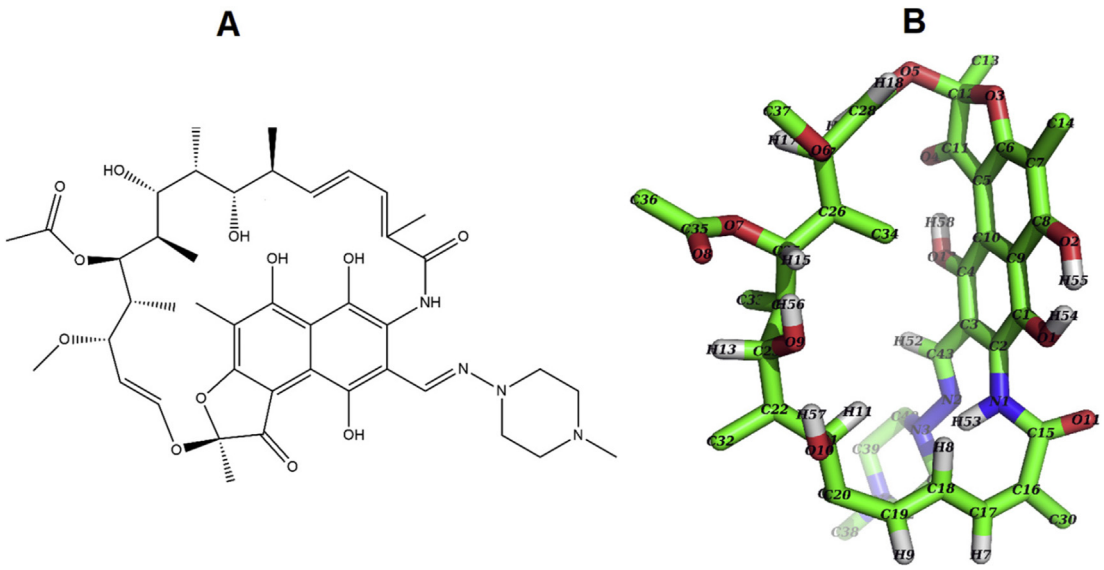

Scheme 1. Chemical structure (A) and three-dimensional structure of RF molecule (B).

on phospholipid nanoparticles are inherently biocompatible, provide improved bioavailability for poorly soluble drugs, and can enable a reduced dose level due to sustained drug release. Even more effective nanodrug delivery systems with nanosized dimensional parameters such as nanoliposomes and micelles are used for the effective local therapeutic release, reducing the overall dose level, and shortening the treatment period [7,8]. Phospholipid nanoparticles are excellent drug delivery systems and efficient carrier of bioactive compounds because of their improved drug solubilization, comfort intravenous injections, long shelf life, easy preparation and improved bioavailability in comparison with solid forms and emulsions [9–11]. RF embedded into phospholipid nanoparticles (NRF) from soy phosphatidylcholine with the addition of sodium oleate was prepared according to technology that was elaborated earlier [10,11]. Incorporation of RF into phospholipid-oleate nanoparticles as delivery system increases its antituberculosis specific activity both in intraperitoneal and in intravenous administration [11]. Pharmacological studies demonstrated a higher bioavailability of NRF than the free drug substance RF. In experiments performed on *M. tuberculosis H37Rv* cells, RF in nanoparticles more actively inhibited cell growth than the free drug substance [10,11].

DNA plays the key role in transcription, translation, replication and division processes. From pharmacological viewpoint, DNA is the most significant target of many medicinal preparations with different biochemical activity. DNA is the main participant of controlled preservation of genetic information, expression and pharmacological target for many cytotoxic and therapeutic agents. From this viewpoint, DNA sensing and drug-DNA interactions are a very important area not only for investigation of pharmacological mechanisms of therapeutic agents and drug discovery but also for understanding of the drug-DNA interaction at the level of genomics and proteomics [12]. The binding of drug molecules to or onto DNA can dramatically change the properties of DNA, leading to disruption in the whole genome functioning. The investigation of the drug-DNA interactions is an important part of rational drug design used for the construction of new and more efficient therapeutic agents and prediction of drug influence on genomic processing. Understanding of mechanism of the drug (or small molecules as candidates for drugs)-DNA interactions can better explain therapeutic efficiency and clinical diagnostics. Hence, understanding of how drug molecules interact with DNA has become an active research area at the interface between synthetic chemistry, genetics, molecular biology and medicine.

Different techniques have been employed for the investigation of drug-DNA complexes including luminescence, fluorescence, spectrophotometry, electrophoresis, liquid and gas chromatography and electrochemical methods based on response of the purine nucleobases, guanine and adenine, after the interaction of DNA with drug molecules [13–15]. The electrochemical studies of the drug-DNA interactions utilize electrodes with a surface-attached DNA, keeping the advantage of specificity, simplicity at operation, rapid response, potential miniaturized platform, low power requirement, and relatively low cost of the analysis [16–21]. Nanocomposite polymeric materials are one of the most widely used supports to enhance electroanalytical sensitivity of biosensors towards DNA molecule [22–28].

The phenomenon of intercalation involves the hydrophobic interaction of drug (usually aromatic part of molecule) with heterocyclic bases, and electrochemistry is a convenient tool to investigate the intercalation of drugs with DNA. However, the comparative investigation of direct interaction of native double-stranded DNA (dsDNA) with RF and particularly with newly developed NRF has not been investigated in detail.

We herein present the first study on comparative effects of RF and NRF on the subsequent DNA-drug interaction. We used quantitative electrochemical analysis of dsDNA *via* direct electrochemical oxidation of guanine and adenine residues, which we published previously elsewhere [21–23,29] and applied this technique for the investigation of the interactions of RF or NRF with dsDNA. For this purpose, we used recently developed modification of screen-printed electrodes (SPEs) with stable fine dispersions of MWCNTs in aqueous solutions of poly(1,2-butadiene)-*block*-poly (2-(dimethylamino)ethyl methacrylate) (PB_{290}-*b*-$PDMAEMA_{240}$) diblock copolymer [22]. By this method, we probed RF-dsDNA or NRF-dsDNA interaction by monitoring the electrochemical oxidation of guanine and adenine nucleobase signals. Such performance was evaluated for observation of both guanine (~0.6 V) and adenine (~0.9 V) oxidation signals response on drug interaction with dsDNA molecule.

2. Experimental

2.1. Materials

MWCNTs with a mean diameter of 9.5 nm and a length of 1 μm were obtained from Sigma-Aldrich. The poly(1,2-butadiene)-*block*-poly(2-(dimethylamino)ethyl methacrylate) (PB_{290}-*b*-$PDMAEMA_{240}$) diblock copolymer was synthesized as described earlier [23]. Fish-sperm double-stranded DNA (dsDNA) as lyophilized powder was obtained from Sigma-Aldrich. All other chemicals were of analytical grade and used without further purification. All aqueous solutions were prepared using Milli-Q water (18.2 MΩ×cm) purified with a Milli-Q water purification system by Millipore.

RF drug substance was obtained from Sandoz Pvt Ltd, India. Rifampicin composition incorporated in phospholipid-oleate nanoparticles (phospholipid-based rifampicin drug delivery system, nanosomal rifampicin), NRF, was prepared in accordance with [10–12].

The stock solution of dsDNA (1.5 mg/mL) was prepared in 100 mM potassium phosphate buffer with 50 mM NaCl (pH 7.4) as described previously [21]. The purity of the dsDNA stock solution was checked by taking the absorbance ratio of A_{260}/A_{280}, which was found to be in the range of 1.8–1.9 indicating there is no proteins contamination in dsDNA solution [24]. The dsDNA stock solution was stored at −20 °C for further use. The stock 10 mM solution of RF was prepared by dissolving it in ethanol. The RF solutions were freshly prepared each day and were always kept protected in the dark to prevent any light-induced changes. NRF was prepared by dissolving lyophilized powder in 100 mM potassium phosphate buffer with 50 mM NaCl (pH 7.4) at the initial concentration of 10 mM. UV–visible absorption spectroscopy was used for the determination of the drug concentration in probe.

2.2. Dispersing of carbon nanomaterials

Aqueous solution of PB_{290}-*b*-$PDMAEMA_{240}$ diblock copolymer was prepared at a concentration of 5 g/L by its direct dissolution in acidified water at pH 3, at which all DMAEMA monomer units of the diblock copolymers are protonated. To disperse carbon nanomaterials, a portion of MWCNTs was added to an aqueous solution of the diblock copolymer in such a way that each 1 mL of the (PB_{290}-*b*-$PDMAEMA_{240}$ + MWCNTs) mixture contained 1.0 mg of the carbon nanomaterial. Then, the mixture was sonicated in Ultrasound Desintegrator SONOPULS HD 4100, 100 W at 30% power in pulse regime for 30 min. Transmission Electron Microscopy (TEM) and Scanning Electron Microscopy (SEM) characteristics of dispersion of MWCNTs in aqueous solution of polycationic PB_{290}-*b*-$PDMAEMA_{240}$ and SPEs modification with PB_{290}-*b*-$PDMAEMA_{240}$/MWCNT dispersions were published elsewhere [22].

2.3. Preparation of electrochemical sensors

Three-pronged SPEs purchased from Color Electronics (Russia, http://www.colorel.ru) were used for the electrode preparation. They consist of a round graphite working electrode (2 mm in diameter) surrounded by a graphite ringed auxiliary counter-electrode and an Ag/AgCl reference electrode. For the preparation of modified electrodes, 2 μL of the aqueous PB_{290}-*b*-$PDMAEMA_{240}$/MWCNT dispersion was dropped onto the working electrode and incubated for 15 min at 37 °C until complete drying. Such modified electrodes were stored refrigerated at +4 °C until measurement on the same day.

For further incorporation of the dsDNA, 60 μL of the dsDNA solution with a specified concentration prepared in 100 mM potassium phosphate buffer with 50 mM NaCl (pH 7.4) was dropped onto the surface of modified electrode and incubated for 15 min before measurements. Horizontal regimen of measurement was used for all experiments.

For the investigation of the drug-dsDNA interaction, a complex of dsDNA with RF or NRF was formed at specified concentrations and was incubated 15 min before adsorption onto electrode surface [15]. DPV measurements were performed after a deposition time of 60 s.

2.4. Electrochemical measurements

Electrochemical measurements were performed using a potentiostat/galvanostat Autolab PGSTAT 12 Autolab (Metrohm Autolab, The Netherlands) operated by the GPES software (version 4.9.7). All electrochemical measurements were carried out at room temperature in 100 mM potassium phosphate buffer with 50 mM NaCl as supporting electrolyte, pH 7.4 (PBS).

The DPV technique was employed in order to follow direct electrochemical oxidation of dsDNA. The following DPV parameters were used: potential range of 0.2–1.2 V, pulse amplitude of 0.025 V, potential step of 0.005 V, pulse duration of 50 ms, modulation amplitude of 0.05 V. All potentials were referred to the Ag/AgCl reference electrode.

Triplicated measurements have been performed for electrochemical estimation of varying concentrations of dsDNA. These values were within 10–12% (the relative standard deviation, RSD = 10–12%) that highlights the inherent repeatability of the setup.

3. Results and discussion

DNA is a natural polyanionic heteropolymer. For this reason we employed a polycationic poly(1,2-butadiene)-*block*-poly(2-(dimethylamino)ethyl methacrylate) (PB_{290}-*b*-$PDMAEMA_{240}$) diblock copolymer, which was used for the preparation of stable aqueous dispersion of MWCNTs. Hereby, the subscripts denote the number-average degrees of polymerization of the respective segment. A highly homogeneous distribution of MWCNTs dispersed in PB_{290}-*b*-$PDMAEMA_{240}$/MWCNT was achieved as was previously confirmed by TEM [22]. The following drop casting of dispersions onto the SPE surface allows complete coverage of the electrode surface with the layer of well-dispersed MWCNTs according to SEM [22]. The results obtained by us earlier convincingly demonstrate that the modification of the SPEs by PB_{290}-*b*-$PDMAEMA_{240}$/MWCNT dispersions results in considerable facilitation of the electron transfer between redox probe and the electroactive electrode surface [22]. In addition, a nearly 7-fold increase in electroactive surface area for the modified SPEs was found. The beneficial effect of the electrode modification of shuch a type was used for the detection of cardiac myoglobin [23] and for studying drug analysis and their conversion by cytochrome P450 3A4 [22].

Prepared as described above, the SPE/PB_{290}-*b*-$PDMAEMA_{240}$/MWCNT modified electrodes were ready to use for direct electrochemical oxidation of DNA. The solutions of dsDNA were prepared in 100 mM potassium phosphate with 50 mM NaCl at physiological pH value of 7.4 and were directly deposited onto the surface of the SPE/PB_{290}-*b*-$PDMAEMA_{240}$/MWCNT modified electrodes. A strong multipoint anchoring of the negatively charged dsDNA at chosen pH value was provided by the electrostatic interaction with partially protonated amino groups of the PDMAEMA block (the protonation degree of PDMAEMA corresponds to about 50% at pH 7.4 in the presence of 100 mM of NaCl in accordance with data of potentionetric titration published elsewhere [23,30]).

DNA electrochemical oxidation was successively realized on the surface of SPE/PB_{290}-*b*-$PDMAEMA_{240}$/MWCNT after deposition of DNA solution on the surface of the modified electrodes. The extensive potential window in the positive direction allows sensitive electrochemical detecting of dsDNA conformational/structural changes. We monitor the concentration-dependent appearance of the oxidation peaks of the DNA components, such as purine bases guanine (G) and adenine (A) registered at ca. ~0.6 V and ca. ~0.9 V, respectively (Fig. 1A-C).

The analytical parameters were determined from the corresponding calibration curves (Fig. 1B, 1C) and are summarized in Table 1. The relative standard deviation (SD) was assessed for at least three measurements ($n \geq 3$) at each concentration level and was found to be within 10%. These results demonstrate that the registration/quantification of dsDNA with the electrodes modified by PB_{290}-*b*-$PDMAEMA_{240}$/MWCNT composite is reproducible, sensitive and comparable with that of the recently reported modified electrodes, which have been used for registration of purine nucleobases of DNA [12,21,29].

We showed that SPE/PB_{290}-*b*-$PDMAEMA_{240}$/MWCNT allows detecting of dsDNA with good sensitivity based on two peaks corresponding to the oxidation of G and A residues at E = 0.591 and E = 0.874 (vs. Ag/AgCl), respectively. Hence, the simultaneous registration of both nucleobases G and A can be used for electrochemical monitoring of RF-dsDNA of NRF-dsDNA interactions based on two active participants of binding events.

Prior to be focused on electrochemical monitoring of the interaction of RF and NRF with dsDNA based on electrooxidation signals of both purine nucleobases, we examined the electrochemical behavior of RF and NTR on the SPE/PB_{290}-*b*-$PDMAEMA_{240}$/MWCNT electrode without DNA.

While the electrochemical behavior of RF itself was studied earlier in details [31,32], the electrochemistry of NRF has been not reported yet. Rifampicin embedded into phospholipid micelles (NRF) from soy phosphatidylcholine with the addition of sodium oleate was prepared according to method that was elaborated earlier [10,11]. Phospholipid nanoparticles with average diameter of 26 ± 3 nm were stable with ζ-potential of −25.0 ± 1.3 mV [10,11]. It was shown that the encapsulation of RF increases its antituberculosis specific activity both in intraperitoneal and in intravenous administration [11]. Pharmacological studies demonstrated a higher bioavailability of NRF than the free drug substance RF. In experiments performed on *M. tuberculosis H37Rv* cells, RF in nanoparticles more actively inhibited cell growth than the free drug substance [10,11].

We used the drug concentrations range of 25–600 μM for the investigation of the interaction of native dsDNA with RF or NRF. It is worth noting that the DPV of RF and NRF itself did not demonstrate any signals in the 0.2–1.2 V potential window and did not notably change background signals in the similar concentration range (Fig. 2). The only adverse effect of RF we have found was a notable increase in the background current at a rather high RF concentration of 700 μM (Fig. 2). Hence, both RF and NRF do not induce any electrochemical interference with dsDNA electrochemical oxidation if their concentration is below about 700 μM. Such electrochemical behaviour for RF can be explained by the chemical structure of this molecule (Scheme 1). Tertiary nitrogen is protonated at physiological pH, so the binding with the polycationic polymer PB_{290}-*b*-$PDMAEMA_{240}$ is not favourable.

Further, the efficacy of RF and NRF binding to dsDNA was studied to compare the interaction mode of both forms of this drug. Based on SPE/PB_{290}-*b*-$PDMAEMA_{240}$/MWCNT modified electrodes,

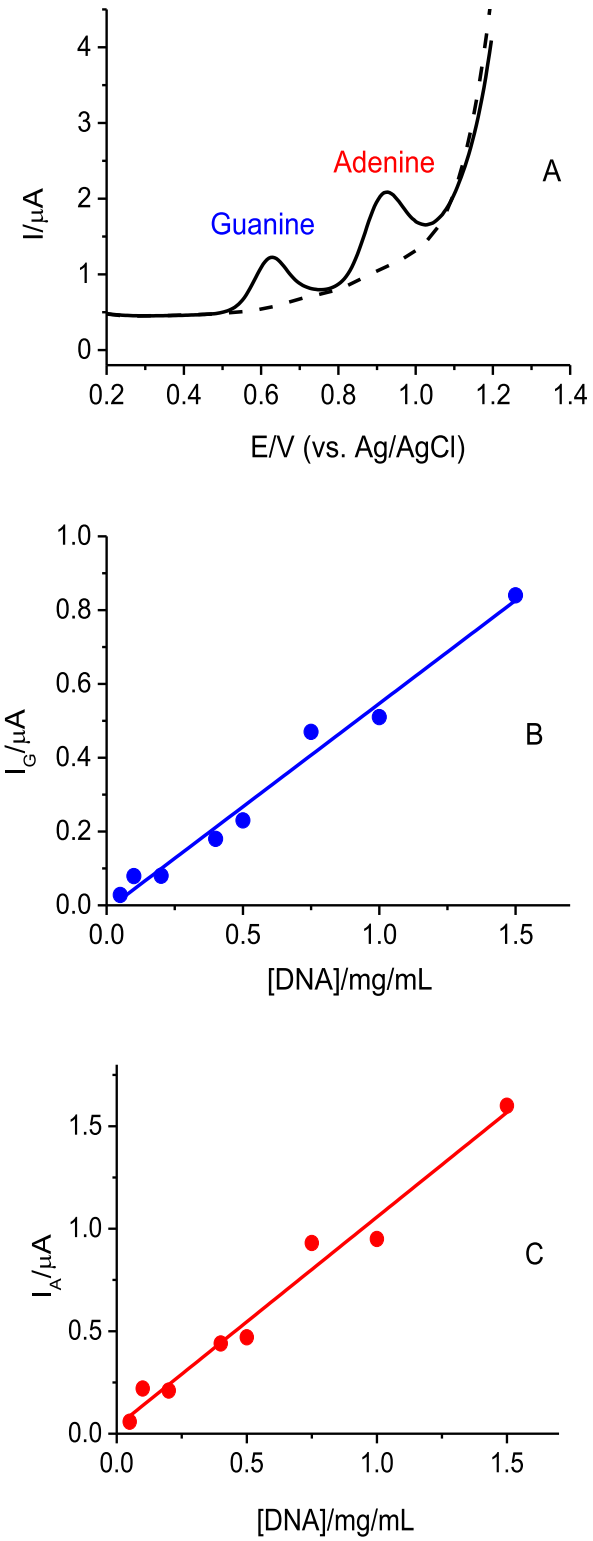

Fig. 1. (A) The typical DPV scans obtained for a bare SPE/PB_{290}-*b*-$PDMAEMA_{240}$/MWCNT (dashed line) and for a SPE/PB_{290}-*b*-$PDMAEMA_{240}$/MWCNT after deposition of 1.5 mg/mL solution of dsDNA (solid line). (B) Oxidative peak current I_G of guanine (G) residues at E = 0.591 V *versus* the concentration of dsDNA for the SPE/PB_{290}-*b*-$PDMAEMA_{240}$/MWCNT; Equation for the linear fit: I_G = 0.559[DNA] − 0.012; R^2 = 0.980; (C) Oxidative peak current I_A of adenine (A) residues at E = 0.874 V *versus* the concentration of dsDNA for the SPE/PB_{290}-*b*-$PDMAEMA_{240}$/MWCNT; Equation for the linear fit: I_A = 1.022[DNA] + 0.035; R^2 = 0.973.

Table 1
Electroanalytical parameters of the quantitative dsDNA assay with SPE/PB_{290}-*b*-$PDMAEMA_{240}$/MWCNT.

	Guanine (G)	Adenine (A)
E_{ox}, V	0.591 ± 0.052	0.874 ± 0.051
Sensitivity, μA/(μg × mL^{-1} × cm^2)	0.53	1.07
Linear range, μg/mL	50–1500	50–1500
Limit of quantification, μg/mL	50	50
Equation for linear regression*)	I_G = 0.559 [dsDNA] − 0.012	I_A = 1.022 [dsDNA] + 0.035

*) I_G, I_A correspond to the oxidative currents (peak heights) for G- and A-residues, respectively; [dsDNA] is a concentration of dsDNA solution in mg/mL that was deposited onto the working electrode surface area.

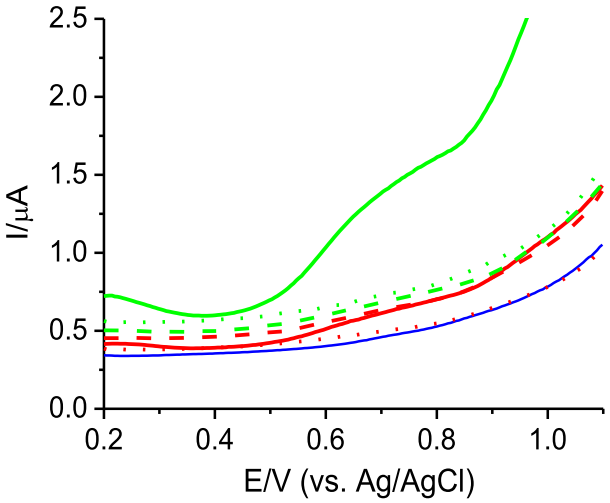

Fig. 2. DPVs of rifampicin (RF) or nanosome/rifampicin (NRF) deposited from solutions with the drug concentration in a range from 50 to 700 μM measured by the SPE/PB_{290}-*b*-$PDMAEMA_{240}$/MWCNT; (blue) 0 μM RF or NRF; (dotted red) 50 μM NRF; (dashed red) 150 μM NRF; (solid red) 700 μM NRF; (dotted green) 50 μM RF; (dashed green) 150 μM RF; (solid green) 700 μM RF.

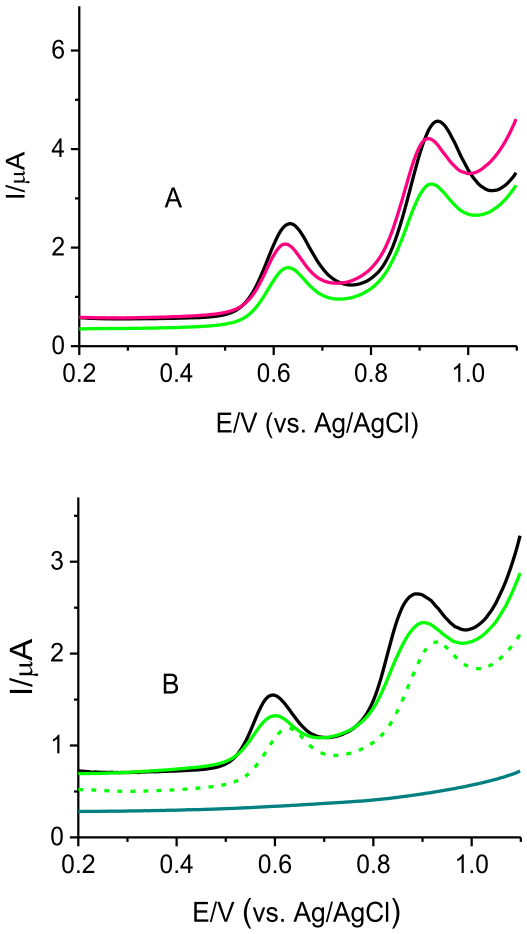

Fig. 3. (A) DPVs of the dsDNA in the absence and in the presence of 25 μM rifampicin (RF) or 25 μM nanosome/rifampicin (NRF); (black) dsDNA, (green) dsDNA + 25 μM RF, (pink) dsDNA + 25 μM NRF. (B) DPVs of dsDNA in the presence of different RF concentrations, (solid black) dsDNA, (solid green) dsDNA + 25 μM RF, (dashed green) dsDNA + 50 μM RF, (solid cyan) 50 μM RF.

we studied the influence of the complexation of dsDNA with RF or NRF on electrochemical signals of G and A oxidation of dsDNA molecule. The interaction of RF or NRF with dsDNA is accompanied by a decrease of DPV oxidation signals of both G and A (Fig. 3A). As can be seen from Fig. 3B, an addition of RF solutions of different concentrations to the dsDNA, results in a clear and pronounced decrease of DPV oxidation signals of both G and A. Additionally, we registered the positive shift of the oxidation potential of G from 0.591 V to 0.630 V and for A from 0.874 V to 0.937 V upon the increasing RF concentration. The same tendencies were found for NRF (Table 2).

Drug toxicity can be estimated at each drug concentration as a value of the percentage of the G or A peak height change (S%) using formula (1) as reported in [15,33] and the dependences of the G or A peak current on drug concentration:

$$S = (S_s/S_b) * 100\%, \quad (1)$$

where S_b and S_s are purine base oxidation signals before and after the drug interaction with dsDNA, respectively. According to the accepted criteria, a drug is considered as nontoxic if S is higher than 85%; the drug is referring to moderately toxic if S is between 50 and 85%, and the drug is toxic if S is below 50% [15,34–36].

The S values were calculated at different RF or NRF concentrations using the G and A peak hights and the results are summarized in Table 2. One can see that NRF demonstrates a considerably less toxic effect upon the interaction with dsDNA than RF. One can also see that the toxic effect of RF/NRF is higher if calculated for A than for G oxidation. Indeed, a moderate toxicity was found for RF in a concentration range of 50–400 μM (for the G peak) or 25–150 μM (for the A peak), while at higher concentrations RF can be considered as toxic. As for NRF, it remained nontoxic up to 500 μM (for the G peak) or up to about 150 μM (for the A peak), while at higher concentrations NRF considered to be moderately toxic.

The voltammetric technique was further used to evaluate the binding constants of RF- or NRF–dsDNA complexes. As the electrooxidation signals of G and A decreased upon RF or NRF addition, titrations with the drug in the range of 20–600 μM were done at a constant dsDNA concentration of 1.5 mg/mL. Electroanalysis of the RF or NRF interaction with dsDNA revealed that no new electrochemical signals appeared after complex formation at the constant DNA concentration and the varying RF or NRF concentration (Fig. 3A. 3B). This feature of electrochemical system based on SPE/PB_{290}-*b*-$PDMAEMA_{240}$/MWCNT permits to use formula for the reversible mode of the interaction of dsDNA and the drug:

$$\text{dsDNA} + \text{drug} \leftrightarrows [\text{dsDNA} * \text{drug}] \quad (2)$$

K_b or the total equilibrium constant can be deduced from this equilibrium as:

$$K_b = [\text{dsDNA} * \text{drug}]/([\text{dsDNA}] \times [\text{drug}]) \quad (3)$$

Table 2
The toxic effects of RF or NRF on dsDNA.

Drug concentration, μM	RF				NRF			
	E_{ox}, V*)		S, %		E_{ox}, V*)		S, %	
	G peak	A peak	G peak	A peak	G peak	A peak	G peak	A peak
0	0.591	0.874	–	–	0.591	0.874	–	–
25	0.596	0.889	85.9	67.7	0.625	0.928	89.4	92.3
50	0.625	0.918	71.4	71.0	0.625	0.932	76.5	76.9
100	0.620	0.918	75.3	70.8	0.630	0.928	87.1	84.6
150	0.625	0.923	65.9	50.5	0.620	0.928	90.6	84.6
400	0.630	0.928	61.2	25.8	0.649	0.962	91.8	76.9
500	0.625	0.923	42.9	29.0	0.644	0.957	87.1	73.1
600	0.630	0.937	25.4	11.8	0.644	0.900	81.2	65.4

*) RSD for E values were 6–8% (n = 3).

We assume that the concentration of dsDNA can be approximated by a peak height calculated either for the A peak or for the G peak. The concentrations of the complexed drug [dsDNA * drug] is assumed to be proportional to the (I_0-I), where I_0 and I are the peak currents of dsDNA in the absence and in the presence of RF or NRF, respectively. Therefore, the equation (3) can be transformed to the equation (4) similarly to the approach described in [35–37]:

$$K_b \approx (I_0 - I)/(I_0 \times ([drug] - (I_0 - I))) \quad (4)$$

The double reciprocal plot of 1/[dsDNA * drug] *vs.* 1/ [drug] is linear and the association binding constant (K_b) is calculated from the ratio of the intercept on the vertical coordinate axis to the slope as described in [35] (Fig. 4). By this way, the binding constants of drug interaction with dsDNA were calculated using the A and G DPV peaks measured in the presence of RF and NRF. The data are summarized in the Table 3.

Using changes in the G oxidation signals, the binding constant K_b for the RF interaction with dsDNA was calculated as 8.56×10^4 M^{-1} and K_b for the NRF was calculated as 1.78×10^3 M^{-1} (Table 3, Fig. 4). Based on the A oxidation signals K_b for both RF and NRF were calculated as 1.48×10^4 M^{-1} and 2.51×10^4 M^{-1}, respectively.

It was shown previously by spectroscopic studies that RF binds to calf-thymus DNA with a binding constant of 5.22×10^5 M^{-1} [5]. The binding constants of molecules that bing to DNA *via* the intercalation mode were reported as $10^4 - 10^6$ M^{-1} [15,37]. Our results on K_b values calculated on the basis of the A signals for RF or NRF allows one to assume the intercalative mode for the drug-dsDNA interaction [5,15,27,37–43]. The values of K_b calculated on the basis of the G signals suggest that RF interacts with dsDNA also *via* intercalation. However, the lower value of K_b for the NRF-dsDNA interaction based on the G signals ($K_b = 1.78 \times 10^3$ M^{-1}) allows us to conclude that NRF cooperates with DNA *via* the electrostatic bonding [15,43–47].

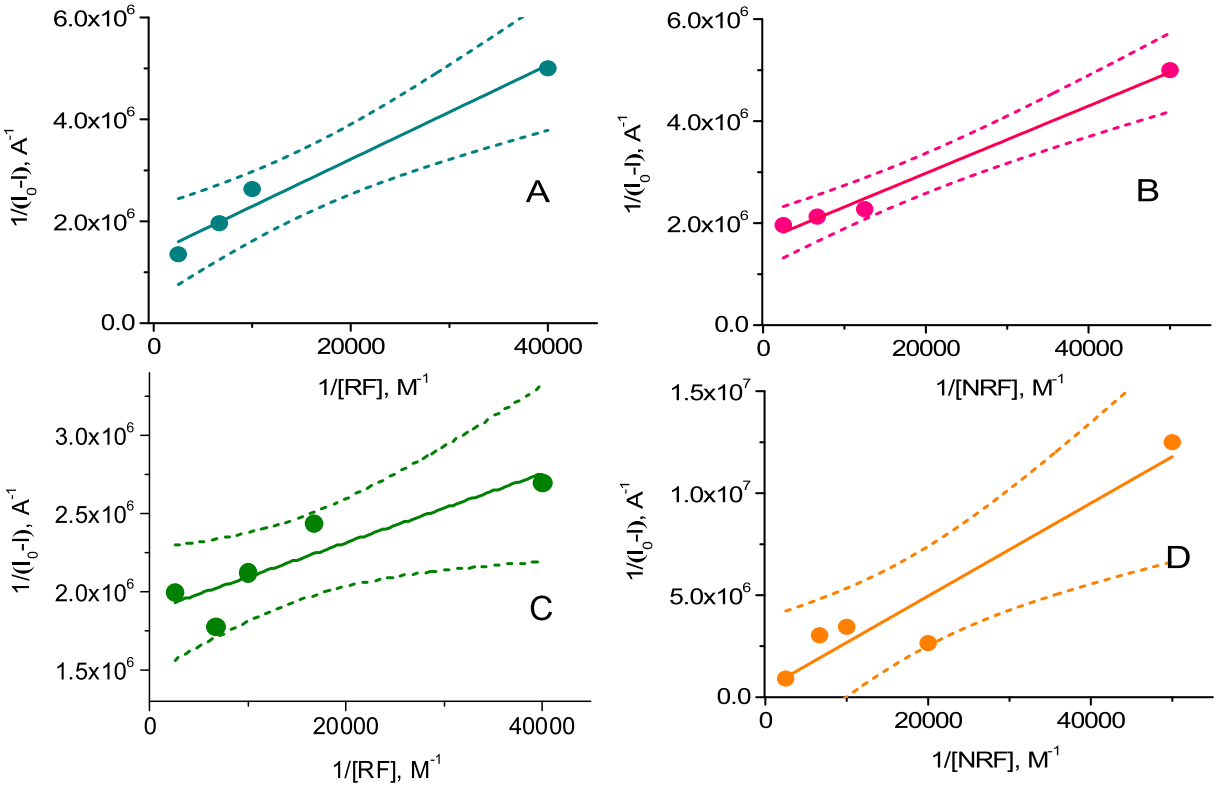

Fig. 4. Linear plots for $1/(I_0 - I)$ depending on 1/[drug]: (A) RF-dsDNA (for the adenine (A) signals); the equation for the linear fit: $y = 92.391x + 1.369 \times 10^6$, $R^2 = 0.964$, $K_b = 1.48 \times 10^4$ M^{-1}; (B) NRF-dsDNA (for the adenine (A) signals); the equation for the linear fit: $y = 66.02x + 1.657 \times 10^6$, $R^2 = 0.984$, $K_b = 2.51 \times 10^4$ M^{-1}; (C) RF-dsDNA (for the guanine (G) signals); the equation for the linear fit: $y = 21.94x + 1.878 \times 10^6$, $R^2 = 0.738$, $K_b = 8.56 \times 10^4$ M^{-1}; (D) NRF-dsDNA (for the guanine (G) signals); the equation for the linear fit: $y = 227.67x + 4.059 \times 10^5$, $R^2 = 0.863$, $K_b = 1.78 \times 10^3$ M^{-1}. Dashed lines show 95% confidence interval.

Table 3
The values of the RF- or NRF–dsDNA binding constants K_b and Gibbs free energy ΔG calculated from the results of the DPV analysis.

Drug-dsDNA complex	K_b, M^{-1}		ΔG = −RTlnK_b, kJ/mol	
	G peak	A peak	G peak	A peak
RF-dsDNA	8.56×10^4	1.48×10^4	−25.8	−21.8
NRF-dsDNA	1.78×10^3	2.51×10^4	−17.0	−23.0

RF as a basket-like molecule with three tertiary protonated nitrogens can also interact with negatively charged phosphate chain, so it is possible to assume that RF (and NRF as well) both interacts *via* intercalation and the electrostatic attraction with the negatively charged DNA. The electrostatic interaction is more pronounced in case of NRF-DNA, which follows from calculations based on decrease of the G oxidation signal.

The change in the Gibbs free energy was calculated on the basis of the binding constants K_b obtained with the electrochemical approach and using the equation ΔG = –RT lnK_b, where R is the universal gas constant, 8.314 J × mol^{-1} × K^{-1}, T is the absolute temperature of 293 K. The calculated values are also summarized in the Table 3. Considerable negative value of ΔG in a range of −17 to −26 kJ/mol were obtained, thereby meaning that binding of RF or NRF to dsDNA represents a thermodynamically favourable process. According to biophysical (circular dichroism CD analysis, competitive displacement experiments and viscosity measurements) and molecular docking studies RF intercalates into the DNA molecule [5,43–48]. As shown earlier, RF binds to the GC-rich region of DNA through multiple hydrogen bonding having the relative binding energy of −9.21 kcal mol^{-1} (−38.56 kJ/mol) [5]. However, with the DPV analysis, we can register the changes in both the G and A oxidation peaks (Fig. 3 B) which might be a notice that RF and NRF interact with both purine nucleobases.

4. Conclusions

Herein, electrochemical technique was applied for the comparative investigation of the interaction of rifampicin, RF, and encapsulated rifampicin, NRF with dsDNA using disposable screen-printed electrodes modified by PB_{290}-*b*-$PDMAEMA_{240}$/MWCNT dispersions. The *in situ* interaction of RF or NRF with dsDNA was monitored by simultaneous measurement of the alteration in both guanine and adenine electrochemical responses. Hence, a more detailed examination of the specific drug-dsDNA binding was carried out with this approach. Indeed, the values of the binding constant K_b were determined separately for the interaction of RF or NRF with adenine or guanine residues. This allows one to get the information on both binding preferences and the type of interaction (more intercalative character in the case of RF-dsDNA interaction or a combination of the intercalation mode and the electrostatic interaction in the case of NRF-dsDNA interaction). This is an obvious advantage of the herein developed electrochemical technique over spectroscopic (optical) sensing where a binding event can be registered just as an integral signal.

At the same time, it is worth nothing that the electrochemical approach might have some limitations. Ideally, a drug should not be an electrochemically active molecule or the oxidative potentials of the interacting molecules should not be overlapped. Otherwise, the electrochemical signals coming from DNA and the drug might interfere. Although the interference might be considerably suppressed when [dsDNA] ≫ [drug].

Thus, such a label-free electrochemical DNA sensing of purine nucleobases is an attractive approach for DNA registration and investigation of DNA-ligand complexes [12,49,50]. The results are of potential use for developing and optimizing drug delivery systems loaded with DNA-targeted molecules for application in chemotherapy, diagnostics, and for an assesment of therapeutic efficacy.

CRediT authorship contribution statement

V.V.S.: conceptualization, methodology, supervision; T.V.B.: investigation, formal analysis; E.G.T.: writing - original draft, writing - review & editing; M.A.S.: data curation; A.V.K.: data curation, validation, formal analysis; R.A.M.: investigation, data curation, validation; D.V.P.: validation, writing - review & editing; F.H.S.: validation, writing - review & editing; L.V.S.: project administration, formal analysis, validation, writing - review & editing.

Declaration of Competing Interest

The authors declare that they have no known competing financial interests or personal relationships that could have appeared to influence the work reported in this paper.

Acknowledgments

This research was supported by the Russian Science Foundation (RSF, project no. 18-44-04011) and the Deutsche Forschungsgemeinschaft (DFG, SCHA1640/18-1) within a joint RSF-DFG grant.

References

[1] H.G. Floss, T.-W. Yu, Rifamycin - mode of action, resistance, and biosynthesis, Chem. Rev. 105 (2005) 621–632, https://doi.org/10.1021/cr030112j.
[2] S. Ramaswamy, J.M. Musser, Molecular genetic basis of antimicrobial agent resistance in *Mycobacterium tuberculosis*: 1998 update, Tuber. Lung Dis. 79 (1998) 3–29, https://doi.org/10.1054/tuld.1998.0002.
[3] K. Asadpour-Zeynali, F. Mollarasouli, Novel electrochemical biosensor based on PVP capped $CoFe_2O_4$@CdSe core-shell nanoparticles modified electrode for ultra-trace level determination of rifampicin by square wave adsorptive stripping voltammetry, Biosens. Bioelectron. 92 (2017) 509–516, https://doi.org/10.1016/j.bios.2016.10.071.
[4] W. Manosuthi, S. Wiboonchutikul, S. Sungkanuparph, Integrated therapy for HIV and tuberculosis, AIDS Res. Ther. 13 (2016) 22, https://doi.org/10.1186/s12981-016-0106-y.
[5] A. Chakraborty, A.K. Panda, R. Ghosh, I. Roy, A. Biswas, Depicting the DNA binding and photo-nuclease ability of anti-mycobacterial drug rifampicin: A biophysical and molecular docking perspective, Int. J. Biol. Macromol. 127 (2019) 187–196, https://doi.org/10.1016/j.ijbiomac.2019.01.034.
[6] R.M. Mainardes, L.P. Silva, Drug delivery systems: past, present, and future, Curr. Drug Targets. 5 (5) (2004) 449–455, https://doi.org/10.2174/1389450043345407.
[7] X. Yuan, R.A. Praphakar, M.A. Munusamy, A.A. Alarfaj, S.S. Kumar, M. Rajan, Mucoadhesive guargum hydrogel inter-connected chitosan-g-polycaprolactone micelles for rifampicin delivery, Carbohydr. Polym. 206 (2019) 1–10, https://doi.org/10.1016/j.carbpol.2018.10.098.
[8] H. Karadeniz, L. Alparslan, A. Erdem, E. Karasulu, Electrochemical investigation of interaction between mitomycin C and DNA in a novel drug-delivery system, J. Pharm. Biomed. Anal. 45 (2007) 322–326, https://doi.org/10.1016/j.jpba.2007.05.005.
[9] X. Ang, H. Chen, J.-Q. Xiang, F. Wei, S.Y. Quek, Preparation and functionality of lipase-catalysed structured phospholipid – A review, Trends Food Sci. Technol. 88 (2019) 373–383, https://doi.org/10.1016/j.tifs.2019.04.005.
[10] O.M. Ipatova, T.I. Torkhovskaya, N.V. Medvedeva, V.N. Prozorovsky, N.D. Ivanova, A.V. Shironin, V.S. Baranova, A.I. Archakov, Bioavailability of oral drugs and the methods for its improvement, Biochem. (Moscow) Suppl. Ser. B: Biomed. Chem. 4 (2010) 82–94, https://doi.org/10.1134/S1990750810010117.
[11] M.A. Sanzhakov, O.M. Ipatova, T.I. Torkhovskaya, E.G. Tikhonova, N.V. Medvedeva, T.S. Zakharova, V.N. Prozorovskiy, The increase of anti-tuberculosis efficacy of rifampicin incorporated into phospholipid

nanoparticles with sodium oleate, Biochem. (Moscow) Suppl. Ser. B: Biomed. Chem. 13 (2019) 271–276, https://doi.org/10.1134/S1990750819030077.
[12] M. Trotter, N. Borst, R. Thewes, F. von Stetten, Review: Electrochemical DNA sensing – Principles, commercial systems, and applications, Biosens. Bioelectron. 154 (2020), https://doi.org/10.1016/j.bios.2020.112069 112069.
[13] E.O. Blair, D.K. Corrigan, A review of microfabricated electrochemical biosensors for DNA detection, Biosens. Bioelectron. 134 (2019) 57–67, https://doi.org/10.1016/j.bios.2019.03.055.
[14] S.T. Girousi, I.C. Gherghi, M.K. Karava, DNA-modified carbon paste electrode applied to the study of interaction between Rifampicin (RIF) and DNA in solution and at the electrode surface, J. Pharm. Biomed. Analy. 36 (2004) 851–858, https://doi.org/10.1016/j.jpba.2004.08.034.
[15] M. Muti, M. Muti, Electrochemical monitoring of the interaction between anticancer drug and DNA in the presence of antioxidant, Talanta 178 (2018) 1033–1039, https://doi.org/10.1016/j.talanta.2017.08.089.
[16] M.R. Arkin, E.D.A. Stemp, C. Turro, N.J. Turro, J.K. Barton, Luminescence quenching in supramolecular systems: a comparison of DNA- and SDS micelle-mediated photoinduced electron transfer between metal complexes, J. Am. Chem. Soc. 118 (1996) 2267–2274, https://doi.org/10.1021/ja9532998.
[17] W. Zhong, J.-S. Yu, Y. Liang, Chlorobenzylidine-herring sperm DNA interaction: binding mode and thermodynamic studies, Spectrochim. Acta A. 59 (2003) 1281–1288, https://doi.org/10.1016/s1386-1425(02)00301-3.
[18] A.M. Oliveira-Brett, V.C. Diculescu, T.A. Enache, I.P.G. Fernandes, A.-M. Chiorcea-Paquim, S.C.B. Oliveira, Bioelectrochemistry for sensing amino acids, peptides, proteins and DNA interactions, Curr. Opin. Electrochem. 14 (2019) 173–179, https://doi.org/10.1016/j.coelec.2019.03.008.
[19] V.K. Sharma, F. Jelen, L. Trnkova, Functionalized solid electrodes for electrochemical biosensing of purine nucleobases and their analogues: a review, Sensors 15 (2015) 1564–1600, https://doi.org/10.3390/s150101564.
[20] P. Das, M. Das, S.R. Chinnadayyala, I.M. Singha, P. Goswami, Recent advances on developing 3rd generation enzyme electrode for biosensor applications, Biosens. Bioelectron. 79 (2016) 386–397, https://doi.org/10.1016/j.bios.2015.12.055.
[21] L.V. Sigolaeva, T.V. Bulko, M.S. Kozin, W. Zhang, M. Köhler, I. Romanenko, J. Yuan, F.H. Schacher, D.V. Pergushov, V.V. Shumyantseva, Long-term stable poly(ionic liquid)/MWCNTs inks enable enhanced surface modification for electrooxidative detection and quantification of dsDNA, Polymer 168 (2019) 95–103, https://doi.org/10.1016/j.polymer.2019.02.005.
[22] V.V. Shumyantseva, T.V. Bulko, A.V. Kuzikov, R.A. Masamrekh, A.Yu. Konyakhina, I. Romanenko, J.B. Max, M. Köhler, A.A. Gilep, S.A. Usanov, D.V. Pergushov, F.H. Schacher, L.V. Sigolaeva, All-electrochemical nanocomposite two-electrode setup for quantification of drugs and study of their electrocatalytical conversion by cytochromes P450, Electrochim. Acta. 336 (2020), https://doi.org/10.1016/j.electacta.2019.135579 135579.
[23] V.V. Shumyantseva, L.V. Sigolaeva, L.E. Agafonova, T.V. Bulko, D.V. Pergushov, F.H. Schacher, A.I. Archakov, Facilitated biosensing *via* direct electron transfer of myoglobin integrated into diblock copolymer/multi-walled carbon nanotube nanocomposites, J. Mater. Chem. B. 3 (2015) 5467–5477, https://doi.org/10.1039/C5TB00442J.
[24] P.G. Held, Nucleic acid purity assessment using A260/A280 ratios. Application Note, BioTek Instruments Incorporation, USA (2001) 1–5.
[25] F. Kuralay, S. Demirci, M. Kiristi, L. Oksuz, A.U. Oksuz, Poly(3,4-ethylenedioxythiophene) coated chitosan modified disposable electrodes for DNA and DNA–drug interaction sensing, Colloids Surf. B. 123 (2014) 825–830, https://doi.org/10.1016/j.colsurfb.2014.10.021.
[26] M. Hasanzadeh, N. Shadjou, Pharmacogenomic study using bio- and nanobioelectrochemistry: Drug–DNA interaction, Mater. Sci. Eng. C. 61 (2016) 1002–1017, https://doi.org/10.1016/j.msec.2015.12.020.
[27] S. Jahandari, M.A. Taher, H. Karimi-Maleh, A. Khodadadi, E. Faghih-Mirzaei, A powerful DNA-based voltammetric biosensor modified with Au nanoparticles, for the determination of Temodal; an electrochemical and docking investigation, J. Electroanal. Chem. 840 (2019) 313–318, https://doi.org/10.1016/j.jelechem.2019.03.049.
[28] I.C. Lopes, A.M. Oliveira-Brett, Human cytochrome P450 (CYP1A2)-dsDNA interaction *in situ* evaluation using a dsDNA- electrochemical biosensor, Electroanal. 29 (2017) 1674–1682, https://doi.org/10.1002/elan.201600713.
[29] L.V. Sigolaeva, T.V. Bulko, A.Yu. Konyakhina, A.V. Kuzikov, R.A. Masamrekh, J.B. Max, M. Köhler, F.H. Schacher, D.V. Pergushov, V.V. Shumyantseva, Rational design of amphiphilic diblock copolymer/MWCNT surface modifiers and their application for direct electrochemical sensing of DNA, Polymers 12 (2020) 1514, https://doi.org/10.3390/polym12071514.
[30] L.V. Sigolaeva, U. Günther, D.V. Pergushov, S.Yu. Gladyr, I.N. Kurochkin, F.H. Schacher, Sequential pH-dependent adsorption of ionic amphiphilic diblock copolymer micelles and choline oxidase onto conductive substrates: Toward the design of biosensors, Macromol. Biosci. 14 (2014) 1039–1051, https://doi.org/10.1002/mabi.201300580.
[31] S. Amidi, Y. Hosseinzadeh Ardakani, M. Amiri-Aref, E. Ranjbari, Z. Sepehri, H. Bagheri, Sensitive electrochemical determination of rifampicin using gold nanoparticles/poly-melamine nanocomposite, RSC Adv. 7 (2017) 40111–40118, https://doi.org/10.1039/c7ra04865c.
[32] S. Shiri, N. Pajouheshpoor, H. Khoshsafar, S. Amidi, H. Bagheri, An electrochemical sensor for the simultaneous determination of rifampicin and isoniazid using a C-dots@CuFe2O4 nanocomposite modified carbon paste electrode, New J. Chem. 41 (2017) 15564–15573, https://doi.org/10.1039/c7nj03029k.
[33] G. Bagni, D. Osella, E. Sturchio, M. Mascini, Deoxyribonucleic acid (DNA) biosensors for environmental risk assessment and drug studies, Anal. Chim. Acta. 573-574 (2006) 81–89, https://doi.org/10.1016/j.aca.2006.03.085.
[34] A. Erdem, M. Muti, P. Papakonstantinou, E. Canavar, H. Karadeniz, G. Congur, S. Sharma, Graphene oxide integrated sensor for electrochemical monitoring of mitomycin C-DNA interaction, Analyst. 137 (2012) 2129–2135, https://doi.org/10.1039/C2AN16011K.
[35] S. Nafisi, A.A. Saboury, N. Keramat, J.-F. Neault, H.-A. Tajmir-Riahi, Stability and structural features of DNA intercalation with ethidium bromide, acridine orange and methylene blue, J. Mol. Struct. 827 (2007) 35–43, https://doi.org/10.1016/j.molstruc.2006.05.004.
[36] E. Eksin, E. Zor, A. Erdem, H. Bingol, Electrochemical monitoring of biointeraction by graphene-based material modified pencil graphite electrode, Biosens. Bioelectron. 92 (2017) 207–214, https://doi.org/10.1016/j.bios.2017.02.016.
[37] L. Fotouhi, F. Bahmani, MWCNT modified glassy carbon electrode: probing furazolidone-DNA interactions and DNA determination, Electroanal. 25 (2013) 757–764, https://doi.org/10.1002/elan.201200495.
[38] K. Morawska, T. Popławski, W. Ciesielski, S. Smarzewska, Electrochemical and spectroscopic studies of the interaction of antiviral drug Tenofovir with single and double stranded DNA, Bioelectrochem. 123 (2018) 227–232, https://doi.org/10.1016/j.bioelechem.2018.06.002.
[39] M. Sirajuddin, S. Ali, A. Badshah, Drug–DNA interactions and their study by UV–Visible, fluorescence spectroscopies and cyclic voltammetry, J. Photochem. Photobiol. B: Biol. 124 (2013) 1–19, https://doi.org/10.1016/j.jphotobiol.2013.03.013.
[40] B. Dogan-Topal, B. Bozal-Palabiyik, S.A. Ozkan, B. Uslu, Investigation of anticancer drug lapatinib and its interaction with dsDNA by electrochemical and spectroscopic techniques, Sens. Actuators B Chem. 194 (2014) 185–194, https://doi.org/10.1016/j.snb.2013.12.088.
[41] Y. Temerk, M. Ibrahim, H. Ibrahim, M. Kotb, Interactions of an anticancer drug lomustine with single and double stranded DNA at physiological conditions analysed by electrochemical and spectroscopic methods, J. Electroanal. Chem. 769 (2016) 62–71, https://doi.org/10.1016/j.jelechem.2016.03.020.
[42] S. Bi, H. Zhang, C. Qiao, Y. Sun, C. Liu, Studies of interaction of emodin and DNA in the presence of ethidium bromide by spectroscopic method, Spectrochim. Acta A. 69 (2008) 123–129, https://doi.org/10.1016/j.saa.2007.03.017.
[43] Z. Yazan, D.E. Bayraktepe, E. Dinç, Four-way parallel factor analysis of voltammetric four-way dataset for monitoring the etoposide-DNA interaction with its binding constant determination, Bioelectrochemistry 134 (2020) 107525, https://doi.org/10.1016/j.bioelechem.2020.107525.
[44] S. Ponkarpagam, G. Mahalakshmi, K.N. Vennila, K.P. Elango, Multi-spectroscopic, voltammetric and molecular docking studies on binding of anti-diabetic drug rosigiltazone with DNA, Spectrochim. Acta Part A Mol. Biomol. Spectrosc. 234 (2020), https://doi.org/10.1016/j.saa.2020.118268 118268.
[45] A. Chakraborty, A.K. Panda, R. Ghosh, I. Roy, A. Biswas, Depicting the DNA binding and photo-nuclease ability of anti-mycobacterial drug rifampicin: A biophysical and molecular docking perspective, Int. J. Biol. Macromol. 127 (2019) 187–196, https://doi.org/10.1016/j.ijbiomac.2019.01.034.
[46] S.Y. Alraqa, K. Alharbi, A. Aljuhani, N. Rezki, I. Ali, Design, click conventional and microwave syntheses, DNA binding, docking and anticancer studies of benzotriazole-1,2,3-triazole molecular hybrids with different pharmacophores, J. Mol. Struct. 1225 (2021) 129192, https://doi.org/10.1016/j.molstruc.2020.129192.
[47] G. Bolat, Investigation of poly(CTAB-MWCNTs) composite based electrochemical DNA biosensor and interaction study with anticancer drug Irinotecan, Microchem. J. 159 (2020), https://doi.org/10.1016/j.microc.2020.105426 105426.
[48] S. Kurbanoglu, B. Dogan-Topal, E.P. Rodriguez, B. Bozal-Palabiyik, S.A. Ozkan, B. Uslu, Advances in electrochemical DNA biosensors and their interaction mechanism with pharmaceuticals, J. Electroanal. Chem. 775 (2016) 8–26, https://doi.org/10.1016/j.jelechem.2016.05.022.
[49] S. Hasoň, M. Fojta, V. Ostatná, Label-free electrochemical analysis of purine nucleotides and nucleobases at disposable carbon electrodes in microliter volumes, J. Electroanal. Chem. 847 (2019), https://doi.org/10.1016/j.jelechem.2019.113252 113252.
[50] E.E. Ferapontova, DNA electrochemistry and electrochemical sensor for nucleic acids, Ann. Rev. Anal. Chem. 11 (1) (2018) 197–218, https://doi.org/10.1146/annurev-anchem-061417-125811.